

## **STUDY OF THE EFFECTS OF THRUST VECTOR ERRORS ON NONIMPULSIVE ORBITAL TRANSFERS**

**Antônio Delson Conceição de Jesus**

**Universidade Estadual de Feira de Santana – UEFS, Feira de Santana, BA, Brasil**

**Phone/Fax: 55-75-2248085, E-mail: [adj@uefs.br](mailto:adj@uefs.br)**

**Marcelo Lopes de Oliveira e Souza, Antônio Fernando Bertachini de A. Prado**

**Instituto Nacional de Pesquisas Espaciais – INPE, S. José dos Campos, SP, Brasil**

**Phone/Fax: 12-3456201/3456226, E-mail: [marcelo@dem.inpe.br](mailto:marcelo@dem.inpe.br), [prado@dem.inpe.br](mailto:prado@dem.inpe.br)**

### **ABSTRACT**

In this paper we present the first part of a Monte-Carlo analysis of nonimpulsive orbital transfers under thrust errors. This was done as part of an extensive study conducted in three phases. The first phase was the numerical implementation and numerical tests of a nonimpulsive trajectory optimization method. The second phase was an extensive Monte-Carlo analysis on nonimpulsive orbital transfers under thrust errors. The third phase was a first algebraic explanation for some of the numerical relations found in the second phase. This paper emphasizes the first (uniform) part of the second phase. Its main results suggest and partially characterizes the progressive deformation of the trajectory distribution along the propulsive arc, turning 3sigma ellipsoids into banana shaped volumes curved to the center of attraction (we call them “bananoids”) due to the loss of optimality of the actual (with errors) trajectories with respect to the nominal (no errors) trajectory. Such deformations can not be anticipated by covariance analysis on linearized models with zero mean errors which propagate ellipsoids into ellipsoids always centered in the nominal (no errors) trajectory. The results also characterize how close or how far are Monte-Carlo analysis and covariance analysis for those examples.

### **INTRODUCTION**

Most space missions need trajectory/orbit transfers to reach their goals. These trajectories/orbits are reached sequentially through transfers between them by changing their keplerian elements, by firing apogee motors or other sources of force. These thrusts have linear and/or angular misalignments that displace the vehicle with respect to its nominal directions. The mathematical treatment for these deviations can be done in many ways (deterministic, probabilistic, minimax, etc.) (Souza et alli, 1998):

In the deterministic approach, Rodrigues (1991) analyzed the effects of the errors in nonimpulsive thrust on coplanar transfers of a nonpunctual model of a satellite. As such, it is the only work we got considering the attitude motion, the center of mass misalignments, and the reduction of thrust with

use. Santos-Paulo(1998) analyzed the effects of errors in impulsive thrusts on coplanar or noncoplanar transfers of punctual model of a satellite. Other correlated papers are Schultz (1997) and Rocco(1999).

In the probabilistic approach, Porcelli and Vogel (1980) presented an algorithm for the determination of the orbit insertion errors in biimpulsive noncoplanar orbital transfers(perigee and apogee), using the covariance matrices of the sources of errors. Adams and Melton (1986) extended such algorithm to ascent transfers under a finite thrust, modeled as a sequence of impulsive burns. They developed an algorithm to compute the propagation of the navigation and direction errors among the nominal trajectory, with finite perigee burns. Howell and Gordon(1994) also applied covariance analysis to the orbit determination errors and they developed a station-keeping strategy of Sun-Earth L1 libration point orbits. Junkins (1997) discussed the precision of the error covariance matrix method through nonlinear transformations of coordinates. He also found a progressive deformation of the initial ellipsoid of trajectory distribution (due to gaussian initial condition errors), that was not anticipated by the covariance analysis of linearized models with zero mean errors. Carlton-Wippern (1997) proposed differential equations in polar coordinates for the growth of the mean position errors of satellites (due to errors in the initial conditions or in the drag), by using an approximation of Langevin's equation and a first order perturbation theory. Alfriend(1999) studied the effects of drag uncertainty via covariance analysis.

In the minimax approach: see russian authors, mainly.

However, all these analyses are approximated and motivated an exhaustive numerical but exact analysis (by Monte-Carlo) and a partial algebraic analysis done by Jesus(1999), to highlight and to study effects not taken care previously.

In this work we present the first (uniform) part of a Monte-Carlo analysis of the nonimpulsive orbital transfers under thrust vector errors. The results were obtained for two transfers: the first, a low thrust transfer between high coplanar orbits, used by Biggs (1978, 1979) and Prado (1989); the second, a high thrust transfer between middle noncoplanar orbits (the first one of the EUTELSAT II-F2 satellite) implemented by Kuga et alli (1991).

The simulations were done for both transfers with minimum fuel consumption. The optimization method used by Biggs (1978 and 1979) and Prado (1989) was adapted to the case of transfers with thrust errors. The "pitch" and "yaw" angles were taken as control variables defined by the overall minimum fuel consumption.

The error sources considered were the magnitude errors, the "pitch" and "yaw" direction errors of the thrust vector, as causes of the deviations found in the Keplerian elements of the final orbit. Each deviation was introduced separately along the orbital transfer trajectory. We studied two types of errors for each one of these causes: the systematic/constructional/assembly errors (modeled as random-bias) and the operational errors (modeled as white-noise). The random-bias errors are unknown but constants during all the transfer arc, while the white-noise errors change along the transfer arc. These error sources introduced in the orbital transfer dynamics cause effects in the keplerian elements of the final orbit at the final instant.

In this work we present an statistical analysis of the effects of these errors on the mean of the deviations of the keplerian elements of the final orbit with respect to the reference orbit (final orbit without errors in the thrust vector) for both transfers. The approach for the treatment of the errors was probabilistic, assuming these as having zero mean uniform probability density function.

## **MATHEMATICAL FORMULATION AND COORDINATE SYSTEMS**

The orbital transfer problem studied can be formulated in the following way:

- 1) Globally minimize the performance index:  $J = m(t_0) - m(t_f)$ ;
- 2) With respect to  $\alpha : [t_0, t_f] \rightarrow \mathbb{R}$  ("pitch" angle) and  $\beta : [t_0, t_f] \rightarrow \mathbb{R}$  ("yaw" angle) with  $\alpha, \beta \in C^{-1}$  on  $[t_0, t_f]$ ;
- 3) Subject to the dynamics in inertial coordinates  $X_i, Y_i, Z_i$  of Figure 1:  $\forall t \in [t_0, t_f]$ ,

$$m(t) \cdot \frac{d^2 X}{dt^2} = \frac{-\mu \cdot m(t) \cdot X}{R^3} + F_X \quad (1)$$

$$m(t) \cdot \frac{d^2 Y}{dt^2} = \frac{-\mu m(t) \cdot Y}{R^3} + F_Y \quad (2)$$

$$m(t) \cdot \frac{d^2 Z}{dt^2} = \frac{-\mu \cdot m(t) \cdot Z}{R^3} + F_Z \quad (3)$$

$$F_X = F [\cos \beta \sin \alpha (\cos \Omega \cos \theta - \sin \Omega \cos I \sin \theta) - \cos \beta \cos \alpha (\cos \Omega \sin \theta + \sin \Omega \cos I \cos \theta) + \sin \beta \sin \Omega \sin I] \quad (4)$$

$$F_Y = F [\cos \beta \sin \alpha (\sin \Omega \cos \theta + \cos \Omega \cos I \sin \theta) - \cos \beta \cos \alpha (\sin \Omega \sin \theta - \cos \Omega \cos I \cos \theta) - \sin \beta \cos \Omega \sin I] \quad (5)$$

$$F_Z = F (\cos \beta \sin \alpha \sin I \sin \theta + \cos \beta \cos \alpha \sin I \cos \theta + \sin \beta \cos I) \quad (6)$$

$$m(t) = m(t_0) + \dot{m} \cdot (t - t_0) \text{ , with } \dot{m} < 0 \quad (7)$$

$$F \cong |\dot{m}| \cdot c \quad (8)$$

Or in orbital coordinates (radial R, transversal T, and binormal N) of Figure 1:

$$m(t) \cdot a_R(t) = F \cdot \cos \beta(t) \cdot \sin \alpha(t) - \frac{\mu \cdot m(t)}{R^2(t)} \quad (9)$$

$$m(t) \cdot a_T(t) = F \cdot \cos \beta(t) \cdot \cos \alpha(t) \quad (10)$$

$$m(t) \cdot a_N(t) = F \cdot \sin \beta(t) \quad (11)$$

$$a_R(t) = \dot{V}_R - \frac{V_T^2}{R} - \frac{V_N^2}{R} \quad (12)$$

$$a_T(t) = \dot{V}_T + \frac{V_R V_T}{R} - V_N \dot{I} \cos \theta - V_N \dot{\Omega} \sin I \sin \theta \quad (13)$$

$$a_N(t) = \dot{V}_N + \frac{V_R V_N}{R} + V_T \dot{I} \cos \theta + V_T \dot{\Omega} \sin I \sin \theta \quad (14)$$

$$V_R = \dot{R} \quad (15)$$

$$V_T = R(\dot{\Omega} \cos I + \dot{\theta}) \quad (16)$$

$$V_N = R(-\dot{\Omega} \sin I \cos \theta + \dot{I} \sin \theta) \quad (17)$$

$$\theta = \omega + f \quad (18)$$

4) Given the initial and final orbits, and the parameters of the problem(  $m(t_0), c, \dots$ ).

These equations were obtained by: 1) writing in coordinates of the dexterous rectangular reference system with inertial directions  $OX_i Y_i Z_i$  the Newton's laws for the motion of a satellite  $S$  with mass  $m$ , with respect to this reference system, centered in the Earth's center of mass  $O$ , with  $X_i$  axis toward the Vernal point,  $X_i Y_i$  plane coincident with Earth's Equator, and  $Z_i$  axis toward the Polar Star approximately; 2) rewriting them in coordinates of the dexterous rectangular reference system with radial, transversal, binormal directions  $SRTN$ , centered in the satellite center of mass  $S$ ; helped by 3) a parallel system with  $OX_o Y_o Z_o$  directions, centered in the Earth's center of mass  $O$ ,  $X_o$  axis toward the satellite  $S$ ,  $X_o Y_o$  plane coincident with the plane established by the position  $R$  and velocity  $V$  vectors of the satellite, and  $Z_o$  axis perpendicular to this plane; and helped by 4) the instantaneous keplerian coordinates ( $\Omega, I, \omega, f, a, e$ ). These equations were later rewritten and simulated by using 5) 9 state variables, defined and used by Biggs(1978, 1979) and Prado(1989), as functions of angle  $s$  shown in Figure 2.

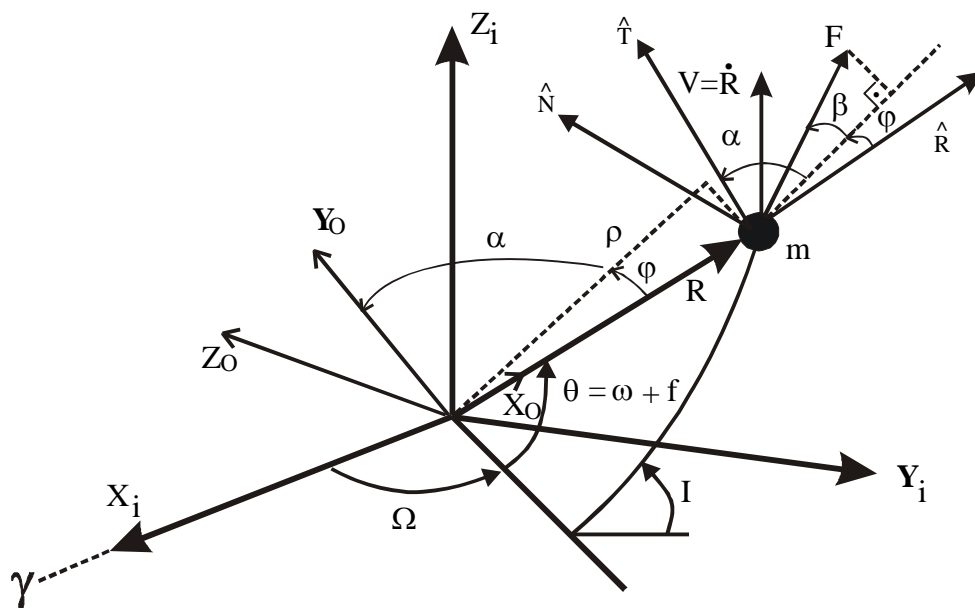


Figure 1 - Reference systems used in this work.

The nonideal thrust vector, with magnitude and direction errors, is given by:

$$\vec{F}_E = \vec{F} + \Delta\vec{F} \tag{19}$$

$$\vec{F}_E = \vec{F}_R + \vec{F}_T + \vec{F}_N \tag{20}$$

$$|\vec{F}_E| = F_E, \quad |\vec{F}| = F \tag{21}$$

$$F_R = (F + \Delta F) \cdot \cos(\beta + \Delta\beta) \cdot \sin(\alpha + \Delta\alpha) \tag{22}$$

$$F_T = (F + \Delta F) \cdot \cos(\beta + \Delta\beta) \cdot \cos(\alpha + \Delta\alpha) \tag{23}$$

$$F_N = (F + \Delta F) \cdot \sin(\beta + \Delta\beta) \tag{24}$$

where:  $\vec{F}$ ,  $\vec{F}_E$  e  $\Delta\vec{F}$  are: the thrust vector without errors, the thrust vector with errors, and the error in the thrust vector, respectively;  $\Delta\alpha$  e  $\Delta\beta$  are the errors in the “pitch” and in the “yaw” angles, respectively;  $F_R$ ,  $F_T$  e  $F_N$  are the components of the thrust vector with errors  $\vec{F}_E$  in the radial, transversal and normal directions, respectively. The magnitude error,  $\Delta F$ , was computed as a percentage of the nominal force, while the direction errors  $\Delta\alpha$  e  $\Delta\beta$  were computed in units of angle. They are varied inside given ranges, that is,  $\pm \text{DES1} \cdot F$  for  $\Delta F$ ,  $\pm \text{DES2}$  for  $\Delta\alpha$  and  $\pm \text{DES3}$  for  $\Delta\beta$ . This variation will correspond to the implementation of the random numbers that satisfy a uniform probability distribution into those ranges. In this way, for each implementation of the orbital transfer arc, values of  $\alpha$  and  $\beta$  are chosen, whose errors are inside the range, that produce the direction for the overall minimum fuel consumption.

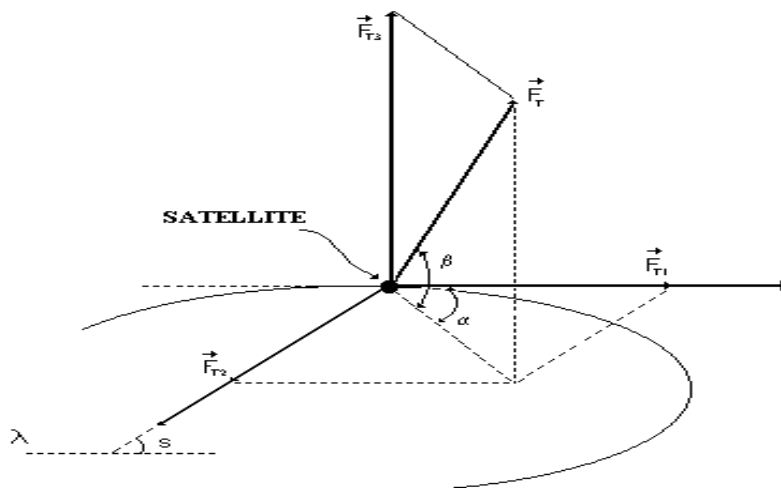


Figure 2 – Thrust vector applied to the satellite and the variable s.

### REFERENCE MANEUVERS USED

The first one came from Example 1, Chapter III of Biggs (1978). The second one came from Kuga et alli (1991). This is the first of three transfer maneuvers of the EUTELSAT II-F2 satellite launched

from Kourou by an Ariane 4 launcher in January 15, 1991 and injected in a gestationary transfer orbit (GTO). Their values are in Tables 1 and 2:

**Table 1: keplerian elements for reference maneuvers used**

Keplerian elements	1 <sup>st</sup> .Maneuver (Biggs, 1978)		2 <sup>nd</sup> .Maneuver (Kuga, 1991)	
	Values at t <sub>0</sub>	Values at t <sub>f</sub>	Values at t <sub>0</sub>	Values at t <sub>f</sub>
Semi-major axis a (km)	99000.000	104000.000	24387.984	27373.907
Eccentricity e	0.7	0.714	0.730044	0.542
Inclination i (deg.)	10.0 <sup>0</sup>	10.0 <sup>0</sup>	6.9948 <sup>0</sup>	3.457 <sup>0</sup>
Ascend. Node Ω (deg.)	55.0 <sup>0</sup>	55.006 <sup>0</sup>	277.4743 <sup>0</sup>	276.265 <sup>0</sup>
Arg. of perigee ω (deg.)	105.0 <sup>0</sup>	104.917 <sup>0</sup>	178.1326 <sup>0</sup>	177.004 <sup>0</sup>
True anomaly f (deg.)	-105.0 <sup>0</sup>	21.213 <sup>0</sup>	200.1568 <sup>0</sup>	189.210 <sup>0</sup>

**Table 2: Common values for reference maneuvers used**

Common values	1 <sup>st</sup> .Maneuver (Biggs, 1978)	2 <sup>nd</sup> .Maneuver (Kuga, 1991)
Thust F (N)	1.0	407.3
Available fuel m(t <sub>0</sub> ) (kg)	2.50	302.691
Exhaust speed c (km/s)	2.5	3.0113
Burn duration t <sub>f</sub> -t <sub>0</sub> (h)	1.700	0.622
Used fuel Δm(t <sub>0</sub> ,t <sub>f</sub> ) (kg)	2.448	289.9867
Initial s s(t <sub>0</sub> ) (deg.)	71.697 <sup>0</sup>	341.318 <sup>0</sup>
Final s s(t <sub>f</sub> ) (deg.)	126.136 <sup>0</sup>	346.718 <sup>0</sup>
Init.pitch angle α (deg.)	-7.793 <sup>0</sup>	-3.516 <sup>0</sup>
Init.yaw angle β (deg.)	0.429 <sup>0</sup>	-25.920 <sup>0</sup>
Init. Pitch rate α̇ (deg./s)	0.889 <sup>0</sup>	2.526 <sup>0</sup>
Init. yaw rate β̇ (deg./s)	-0.006 <sup>0</sup>	6.408 <sup>0</sup>
Initial s step Δs (deg.)	10.0 <sup>0</sup>	5.0 <sup>0</sup>
Number of prop. Arcs	<b>1</b>	<b>1</b>

### NUMERICAL RESULTS

The simulations were performed with 1000 realizations for each transfer, that is, 1000 runs were done with random values for each DES1, DES2 and DES3, such that the results obtained for the final keplerian elements represent the arithmetic mean of 1000 realizations (mean over the ensemble). The value 1000 was chosen to represent the set of runs because the mean deviations in all final keplerian elements with respect to their references converge to their steady state values for this number of runs. Figures 3 and 4 show the mean deviations in the final semi-major axis and eccentricity versus the number of runs, respectively. These plots were done for systematic pitch direction with DES2=1.0<sup>0</sup>. The computation of the mean deviations of the final keplerian elements with respect to their references can be estimated by the arithmetic mean of them, for 1000 runs as representatives. So, we can estimate mean deviation of a final keplerian element, ΔK as,

$$\overline{\Delta K} = E\{\Delta K\} = \int_{-\infty}^{\infty} \xi \cdot f_{\Delta K}(\xi) \cdot d\xi \cong \sum_{i=1}^{N=1000} \frac{\Delta K_i}{N} \quad (25)$$

It is important to remark that Eq. (25) estimates a mean in the ensemble and not in the time. In this work we present only these estimates for the final semi-major axis and eccentricity with respect to

their references. Figures 5 to 16 present the behavior of them as functions of the maximum (random-bias and white noise) **direction errors**. For the random-bias errors we found the following results:

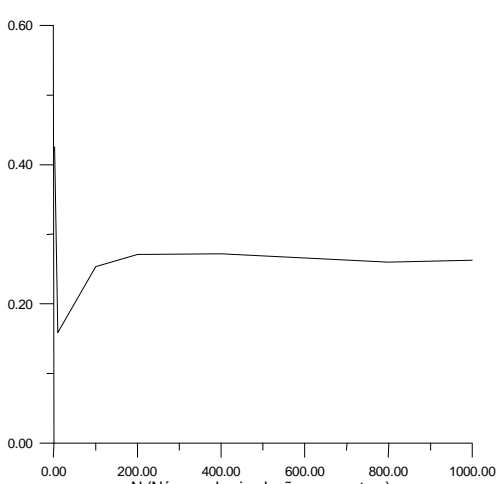


**Figure 3 –Semi-major axis deviation (km) vs. N**

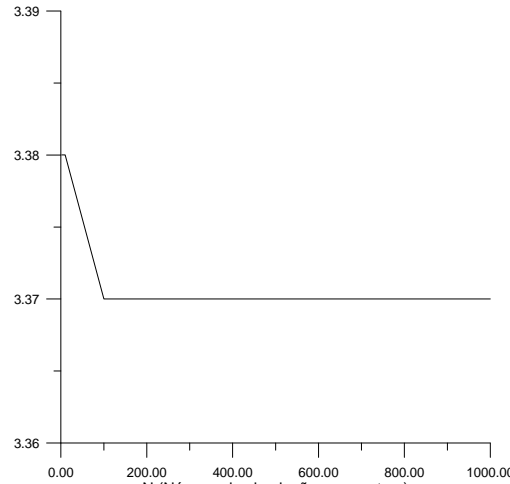


**Figure 4 - Eccentricity deviation ( $\times 10^{-4}$ ) vs. N**

**1) Uniform random-bias errors: semi-major axis (a), “pitch” errors**

We note in Figures 5 and 6, behaviors very similar for both maneuvers, although they are very different from each other. We easily observe that the values of the mean semi-major axis present a region of

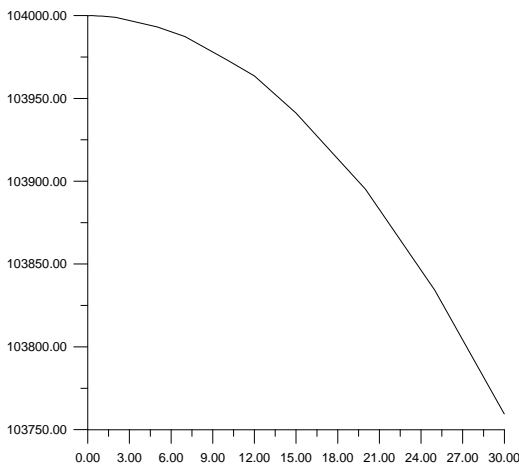


**Figure 5 – First Maneuver:  $E\{a(t_f)\}$  (km) vs DES2 ( $^\circ$ )**

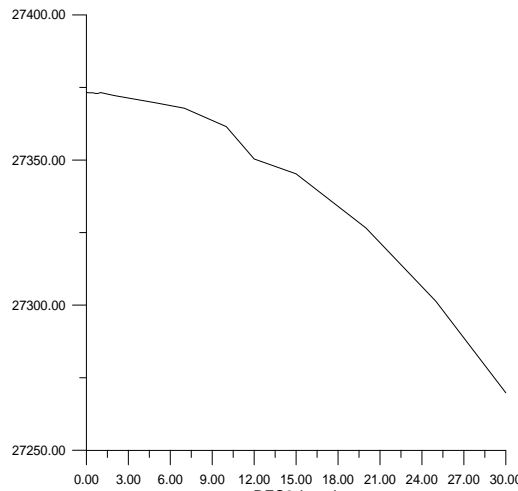


**Figure 6 – Second Maneuver:  $E\{a(t_f)\}$  (km) vs DES2 ( $^\circ$ )**

decrease sufficiently defined according to the growth of the maximum “pitch” error, DES2. Figures 5 and 6 suggest a nonlinear law between these elements for both cases, that is, they suggest a cause vs. effect relation in the orbital transfer phenomenon, not depending of the maneuver studied.

**2) Uniform random-bias errors: semi-major axis (a), “yaw” errors**

Once more Figures 7 and 8 show behaviors well defined and similar for the semi-major axis as function of the maximum “yaw” error, DES3, for both maneuvers studied. That is, there is a region of decrease well defined between the elements  $a$  and DES3. In the second case, the curve found seems to turn itself smoother with respect to the case DES2. This fact is due to the stronger dependence of this

element with DES3. So, we can say that this nonlinear relation between the cause along the transfer and the effect in the final instant also occurs for the out-of-plane maneuvers.

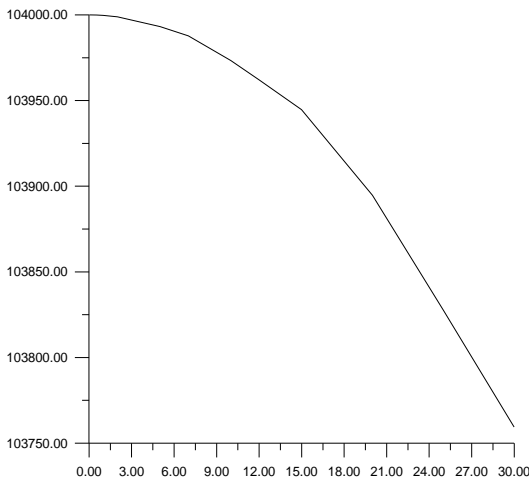


**Figure 7 – First Maneuver:  $E\{a(t_f)\}$  (km) vs DES3 ( $^\circ$ )**

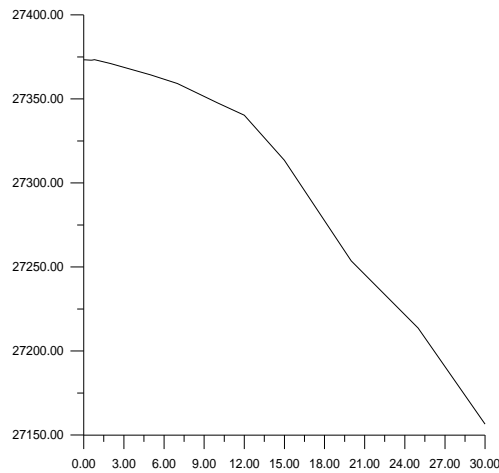


**Figure 8 – Second Maneuver:  $E\{a(t_f)\}$  (km) vs DES3 ( $^\circ$ )**

**3) Uniform random-bias errors: eccentricity (e), “pitch” and “yaw” errors**

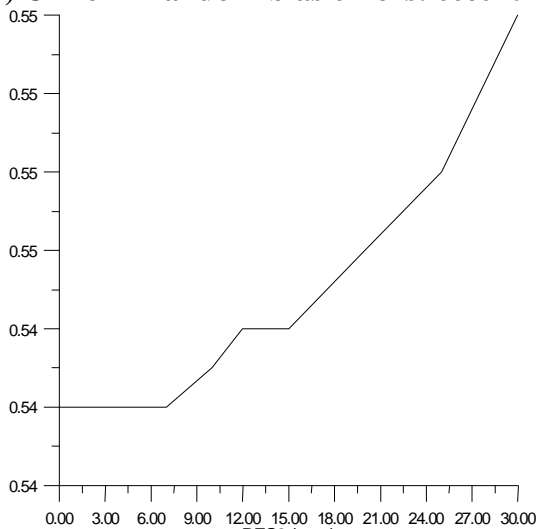


**Figure 9 – Second Maneuver:  $E\{e(t_f)\}$  (km) vs DES2 ( $^\circ$ )**

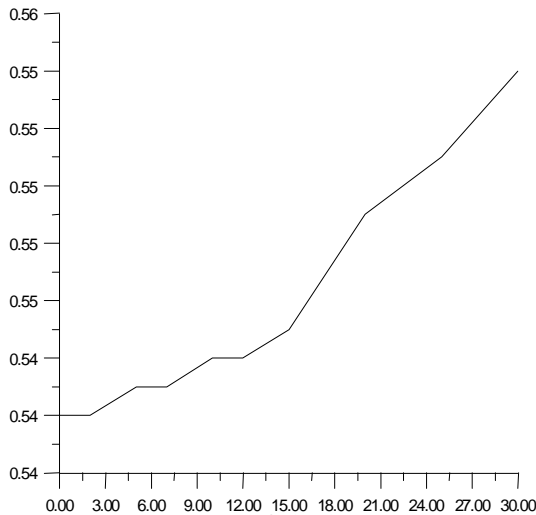


**Figure 10 – Second Maneuver:  $E\{e(t_f)\}$  (km) vs DES3 ( $^\circ$ )**

Figures 9 and 10 show the nonlinear behavior of the mean final eccentricity with the maximum “pitch” and “yaw” deviations. They were done only for the second maneuver because in the first one the change of the eccentricity is close to zero for the usual values of DES2 and DES3. They were plotted with precision of  $10^{-3}$  for the eccentricity.

**5) Uniform white-noise errors: semi-major axis (a), “pitch” errors**

For the white-noise errors Figures 11 and 12 were very similar to the results obtained for the random-bias errors but the curves for the “pitch” errors present a more defined pattern with respect to those for the “yaw” errors, where small fluctuations appear in its final form. It is possible to see that the influence of the out-of-plane (“yaw”) errors is so strong in the definition of the orbital transfer trajectory.



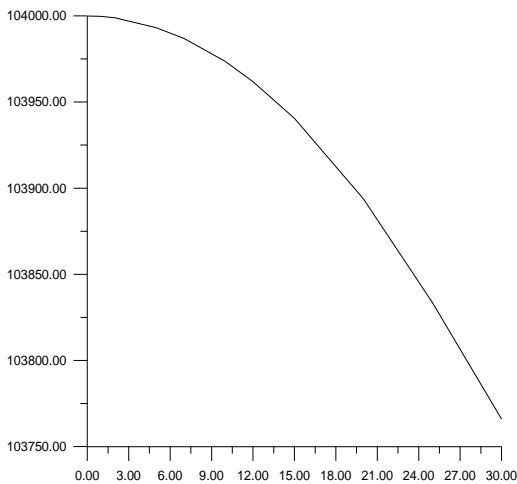


**Figure 11 – First Maneuver:  
E{a(t<sub>f</sub>)} (km) vs DES2 (°)**

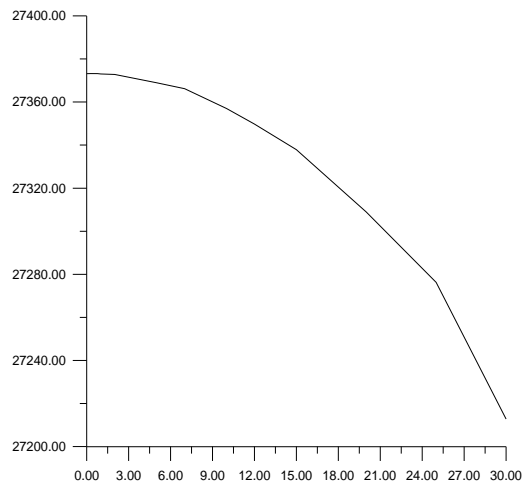


**Figure 12 – Second Maneuver:  
E{a(t<sub>f</sub>)} (km) vs DES2 (°)**

**5) Uniform white-noise errors: semi-major axis (a), “yaw” errors**

Figures 13 and 14 clearly show the influence of the white-noise errors when the second maneuver is simulated with errors in “yaw”. The region of decrease and the nonlinear relation still exist, but there are fluctuations in the growth of the maximum “yaw” error.

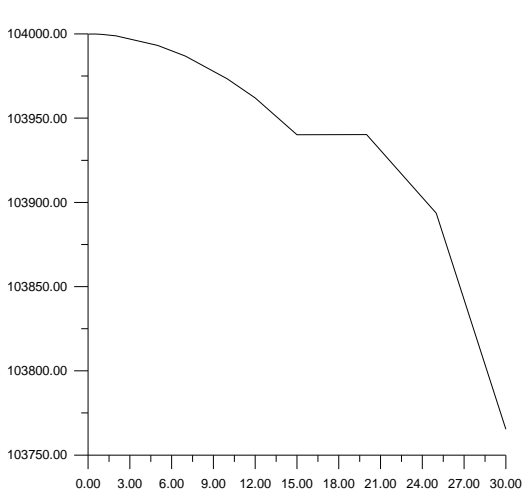


**Figure 13 – First Maneuver: E{a(t<sub>f</sub>)}  
(km) vs DES3 (°)**

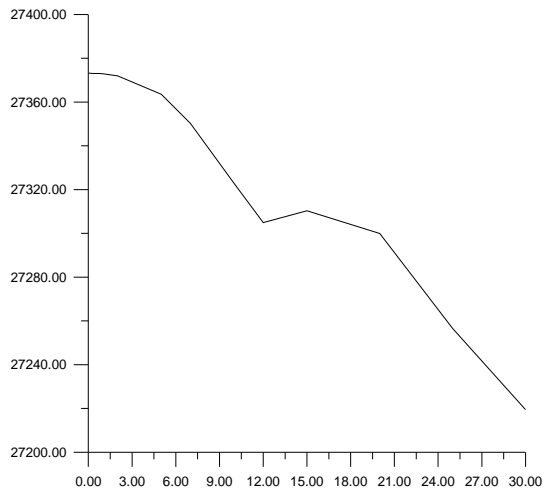


**Figure 14 – Second Maneuver:  
E{a(t<sub>f</sub>)} (km) vs DES3 (°)**

**6) Uniform white-noise errors: eccentricity (e), “pitch” and “yaw” errors**

Figures 15 and 16 show that the values of the eccentricity also fluctuate for practical maneuvers with the white-noise errors in “yaw”, but keeping the region of growth similar to the one verified for the random-bias errors case. So, we can say that all these results suggest and partially characterizes the progressive deformation of the trajectory distribution along the propulsive arc. It occurs due to the loss of optimality of the actual trajectories (with errors) with respect to the nominal trajectories (without errors).

The dependence of the final keplerian elements with the **magnitude errors** for any of the cases was practically null, specially for the mean deviation of the final semi-major axis, since the perturbations occurred in this element were probably due to its estimator and they were comparable to the numerical

errors of the experiment, as shown in Figures 17 and 18. They show that the mean deviation in the final semi-major axis is much smaller than the cone  $\pm 1 \sigma$  (standard deviation of the deviation in the final semi-major axis).

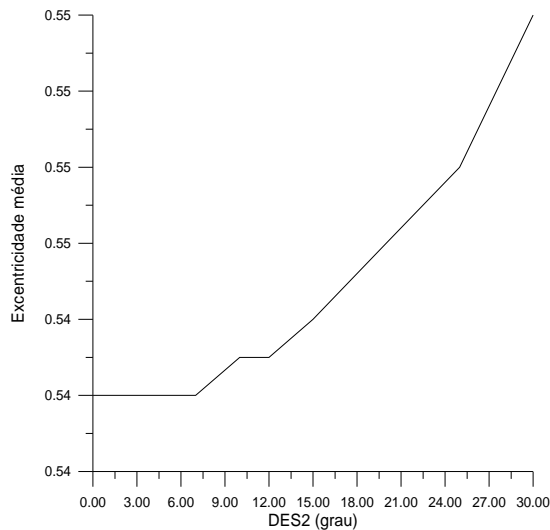


**Figure 15 – Second Maneuver:  $E\{e(t_f)\}$  (km) vs DES2 ( $^\circ$ )**

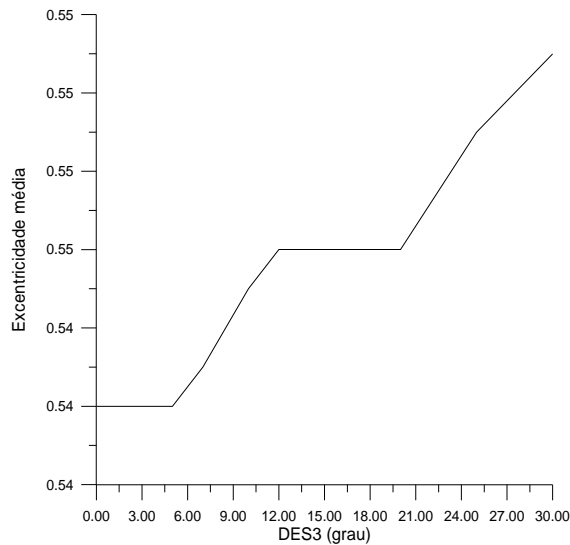


**Figure 16 – Second Maneuver:  $E\{a(t_f)\}$  (km) vs DES3 ( $^\circ$ )**

The values for DES1, DES2 and DES3 used in these plots range from usual values to nonusual values, with the aim to verify the general behaviors. Obviously, it is not usual to have a “pitch” error equal to  $30.0^\circ$  or a magnitude error equal to 30.0%, for example.

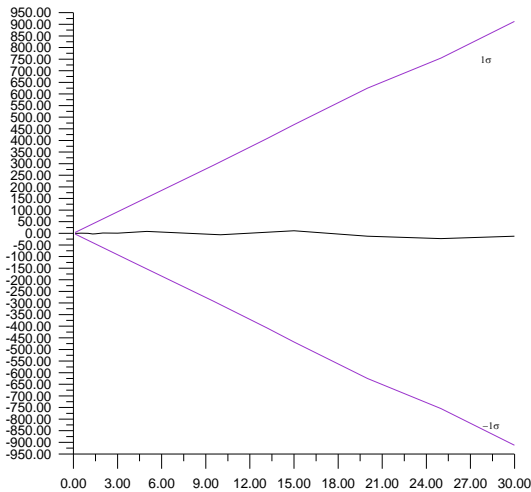


**Figure 17 – First case;  $E\{\Delta a(t_f)\}$  (km) vs DES1 ( $^\circ$ ) and its  $\sigma$  (std.dev.)**

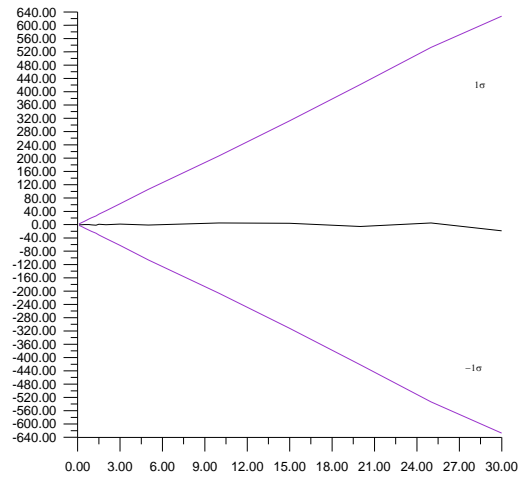


**Figure 18 – 2nd. case;  $E\{\Delta a(t_f)\}$  (km) vs DES1 ( $^\circ$ ) and its  $\sigma$  (std. dev.)**

### CONCLUSIONS

This work presented results of the thrust vector errors implementation for nonimpulsive orbital transfer maneuvers. It was verified that, in any case, the mean deviation in the final semi-major axis presents a nonlinear (approximately parabolic) dependence with the maximum errors in thrust directions. The same results were verified for the mean deviation in the final eccentricity, for the second transfer. The respective dependences with the thrust magnitude errors were not verified. Such

results suggest a progressive deformation of the trajectory distribution along the propulsive arc. This deformation may be associated to the loss of the optimality of the actual trajectories with respect to the nominal trajectory. These results also suggest and partially characterizes the progressive deformation of the trajectory distribution along the propulsive arc, turning 3sigma ellipsoids into banana shaped volumes curved to the center of attraction (we call them “bananoids”) due to the loss of optimality of the actual (with errors) trajectories with respect to the nominal (no errors) trajectory. Such deformations can not be anticipated by covariance analysis on linearized models with zero mean errors which propagate ellipsoids into ellipsoids always centered in the nominal (no errors) trajectory. The results also characterize how close or how far are Monte-Carlo analysis and covariance analysis for those examples.

### ACKNOWLEDGEMENTS

The authors thanks hartly: 1) CAPES/PICDT, Brasil for supporting this work via a 4 year doctoral scholarship to the 1<sup>st</sup>. author; 2) INPE, S.J.Campos, Brasil, for employing the 2<sup>nd</sup> and 3<sup>rd</sup> authors during the work.

### REFERENCES

- Adams, N.J.; Melton, R. G.** “Orbit Transfer Error Analysis for Multiple, Finite Perigee Burn, Ascent Trajectories”. *The Journal of Astronautical Sciences*, 34(4), p.355-373, 1986.
- Alfriend, K. T., K. T., Lee, D. J., Wilkins, M. P.** “Characterizing Orbit Uncertainty Due to Atmospheric Drag Uncertainty”. *Revista Brasileira de Ciências Mecânicas*, vol.XXI, Special Issue, p.182-190, 1999.
- Biggs, M.C.B.** *The Optimisation of Spacecraft Orbital Manoeuvres. Part I: Linearly Varying Thrust Angles*. The Hattfield Polytechnic Numerical Optimisation Centre, Connecticut, USA, 1978.
- Biggs, M.C.B.** *The Optimisation of Spacecraft Orbital Manoeuvres. Part II: Using Pontryagin’s Maximum Principle*. The Hattfield Polytechnic Numerical Optimisation Centre, Connecticut, USA, 1979.
- Carlton-Wippenn, K. C.** *Satellite Position Dilution of Precision (SPDOP)*. AAS Paper 97-609, presented at the 1997 AAS/AIAA Astrodynamics Specialist Conference, Sun Valley, ID, August 4-7, 1997.
- Howell, K.C.; Gordon, S.C.** “Orbit Determination Error Analysis and a Station-Keeping Strategy for Sun-Earth L1 Libration Point Orbits”. *The Journal of Astronautical Sciences*, 42(2), p.207-228, 1994.
- Jesus, A.D.C.** *Análise Estatística de Manobras Orbitais com Propulsão Finita Sujeita a Erros no Vetor Empuxo*. Doctoral Thesis. INPE, S. J. Campos, SP, Brazil, 1999.
- Junkins, J. L.; Akella, M. R.; Alfriend, K. T.** "Non-Gaussian Error Propagation in Orbital Mechanics". *The Journal of the Astronautical Sciences*, 44 (4), October-December, p.541-563, 1996.
- Junkins, J. L.** “Adventures on the Interface of Dynamics and Control”. *Journal of Guidance, Control, and Dynamics*, 20(6), p.1058-1071, 1997.
- Kuga, H. K.; Gill, E.; Montenbruck, O.** *Orbit Determination and Apogee Boost Maneuver Estimation Using UD Filtering*. DLR-GSOC, Wesling, Germany, 1991 (Internal Report DLR-GSOC IB 91-2).

**Porcelli, G; Vogel, E.** "Two-Impulse Orbit Transfer Error Analysis Via Covariance Matrix". *Journal of Spacecraft and Rockets* 17(3), p.248-255, 1980.

**Prado, A.F.B.A.** *Análise, Seleção e Implementação de Procedimentos que Visem Manobras Ótimas de Satélites Artificiais*. Master Dissertation. INPE, S.J. dos Campos, SP, 1989 (INPE-5003-TDL/397).

**Rao, K.R.** "Orbit Error Estimation in the Presence of Force Model Errors". AAS Paper 93-254 in: *Advances in the Astronautical Sciences*, 84(I), p.61-74, 1993.

**Rocco, E.M.** *Manutenção Orbital de Constelações Simétricas de Satélites Utilizando Manobras Impulsivas Ótimas com Limite de Tempo*. (on going) Doctoral Thesis. INPE, S.J. Campos, SP, Brazil, 2000.

**Rodrigues, D.L.F.** *Análise Dinâmica da Transferência Orbital*. Master Dissertation. INPE, S.J. Campos, SP, Brasil, 1991 (INPE-5352-TDI/461).

**Santos-Paulo, M.M.N.** *Estudo de Manobras Tridimensionais Impulsivas pelo Método de Altman e Pistiner, com Erros nos Propulsores*. Master Dissertation. INPE, S.J. Campos, SP, Brazil, 1998.

**Schultz, W.** "Transferências biimpulsivas ente órbitas elípticas não coplanares com consumo mínimo de combustível". Master Dissertation. INPE, S.J. dos Campos, SP, Brazil, 1997.

**Souza, M. L. O., Prado, A. F. B. A., Rodrigues, D. L. F., Santos-Paulo, M. M. N., Jesus A. D. C. and Rocco, E. M.** "A Discussion on the Effects of Thrust Misalignments on Orbit Transfers", *Proceedings of the XXI Congresso Nacional de Matemática Aplicada e Computacional*, Caxambu, MG, Brasil, September 14-18, 1998, p.73.